Chapter 2
Structure and Tectonic Development of the Kinneret Basin

Zvi Ben-Avraham, Michal Rosenthal, Gideon Tibor, Hila Navon, Hillel Wust-Bloch, Rami Hofstetter and Michael Rybakov

Abstract The Sea of Galilee is a freshwater lake in northern Israel, occupying a part of the Lake Kinneret basin along the Dead Sea fault. The basin is located in an area of tectonic complexity, where the main north–south trending segments of the Dead Sea fault intersect with a secondary system of northwest–southeast and east–west trending faults in the Galilee. Plio–Pleistocene basalt flows and intrusions varying in thickness are present around the lake. This tectonic setting produced the complicated sub-bottom structure of the basin. Numerous studies have dealt with this issue using various methods: seismic reflection and refraction, heat flow, bathymetry, magnetics, gravity, and seismicity. This chapter summarizes the findings of the previous and recent studies of the sub-bottom and floor of the lake. The Lake Kinneret basin is composed of two subbasins. The northern subbasin is the most tectonically active zone in the lake and forms the deepest bathymetric part of it. The southern subbasin is the deepest part of the basin, filled with 5–8 km of sediments. Both longitudinal boundary faults and transverse faults are present in the lake; however, their accurate geometry is in dispute. Structural evolution of the

Z. Ben-Avraham (✉) · M. Rosenthal · H. Navon · H. Wust-Bloch
Department of Geophysical, Atmospheric and Planetary Sciences,
Tel Aviv University P.O.B. 39040, 69978 Tel Aviv, Israel
e-mail: zviba@post.tau.ac.il

M. Rosenthal
e-mail: rofemich@post.tau.ac.il

H. Navon
e-mail: hilaweis@post.tau.ac.il

H. Wust-Bloch
e-mail: hillelw@post.tau.ac.il

G. Tibor
Israel Oceanographic & Limnological Research,
P.O.B. 8030, 31080 Haifa, Israel
e-mail: tiborg@ocean.org.il

R. Hofstetter
Geophysical Institute of Israel, P.O.B. 182, 71100 Lod, Israel
e-mail: ramih@gii.co.il

M. Rybakov
e-mail: rybakovmichael6@gmail.com

T. Zohary et al. (eds.), *Lake Kinneret, Ecology and Management,* Aquatic Ecology Series 6,
DOI 10.1007/978-94-017-8944-8_2,

basin is associated with several tectonic processes. The interaction between the two fault systems may have caused rotational opening and transverse normal faulting that formed the northern subbasin. Strike–slip motion along the main segments of the Dead Sea fault is probably responsible for the pull-apart opening of the southern subbasin.

Keywords Active faults · Bathymetry · Dead Sea fault · Gravity · Magnetic · Seismic reflection · Seismic refraction · Volcanism

2.1 Introduction

Lake Kinneret is one of a number of morphotectonic depressions along the Dead Sea fault (Garfunkel 1981; Kashai and Croker 1987; Garfunkel and Ben-Avraham 2001)—a plate boundary of the transform type which connects the Red Sea, where the seafloor spreading occurs, with the Taurus–Zagros zone of continental collision (Fig. 2.1). It is a freshwater lake, 12 km at its widest point and approximately 20 km long. Its surface is approximately 210 m below mean sea level and has a maximum depth of 41.7 m (Chap. 4). Due to high sedimentation rates of 2–7 mm year^{-1} (Serruya 1973; Inbar 1976), the lake floor is relatively flat.

The Lake Kinneret basin is composed of the lake itself and the Kinarot Valley to the south. It forms the northern section of the Kinneret–Beit Shean basin, which began to form during the Neogene (Picard 1943; Schulman 1962; Garfunkel and Ben-Avraham 2001), as a result of the strike–slip motion along the N–S-trending Dead Sea fault. This remains the major fault trend in the basin. However, a secondary NW–SE to W–E-trending fault system composed of branching faults, such as the Carmel fault (Fig. 2.1), exits on the western side of the Dead Sea fault (Saltzman 1964; Freund 1970; Shaliv 1991). This secondary system resulted in reactivation of older systems, creating complicated structures and fault patterns. Braun et al. (2009) suggested a strong coupling of the Carmel fault with the Dead Sea fault, and Sadeh et al. (2012) found that a high fraction of the total slip is being accommodated by the Carmel fault. Farther north, additional faults branch off from the Dead Sea fault (Ron et al. 1984; Heimann 1990) in the region of the Palmyra Range and westward, with the Yammouneh fault being the main branch (Walley 1998).

The structure of Lake Kinneret is complex and results from the intersection of the two fault systems in the area. Superposition of vertical displacements perpendicular or oblique to the N–S transform fault created complicated structures in the area. Because Plio–Pleistocene basalt flows and intrusions vary in thickness, structural interpretation is difficult.

Basalt outcrops are exposed around Lake Kinneret (Fig. 2.2), mainly of the Cover Basalt formation (Picard 1936; Schulman 1962). The maximum thickness of this unit is 175 m (Michelson 1972). K–Ar and Ar–Ar radiometric ages (Siedner and Horowitz 1974; Mor and Steinitz 1982; Mor 1986, 1993; Heimann et al. 1996; Weinstein et al. 2006) indicate that the Cover Basalt is 5.5–3.3 Ma. This age ranges between the Gilbert and the Gauss paleomagnetic eras, each characterized with a different paleomagnetic polarity. Accordingly, the Cover Basalt in the Galilee is

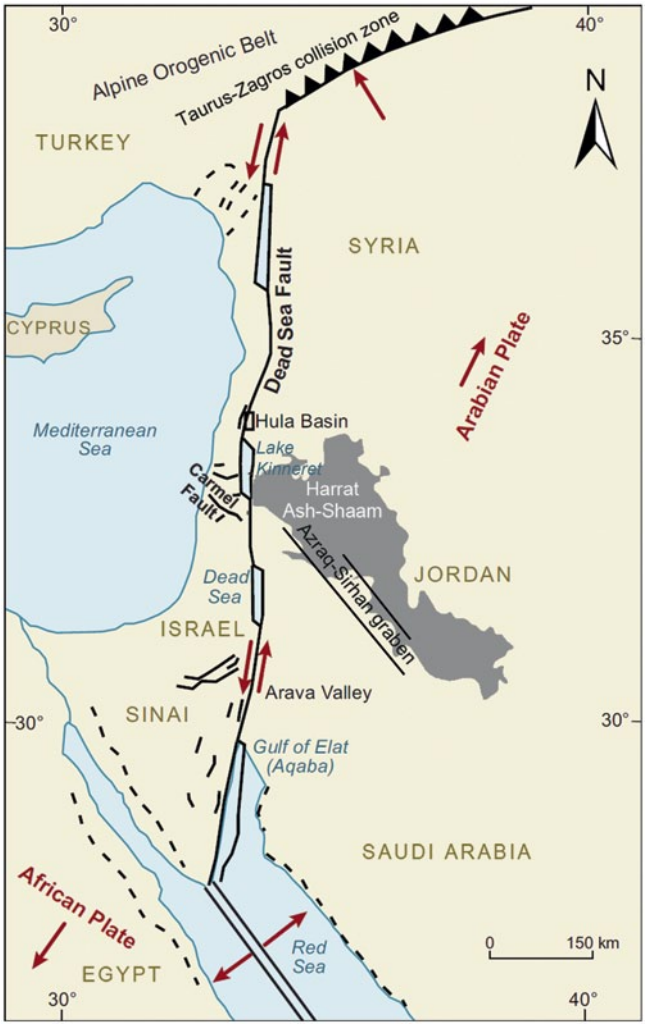

Fig. 2.1 Regional setting of the Dead Sea fault zone and the Carmel fault system (tectonic features are schematic). (Modified with permission after Ben-Avraham et al. 2008)

normally magnetized in the lower part and reversely magnetized in the upper part (Freund et al. 1965). However, in the Golan Heights, the whole Cover Basalt section is reversely magnetized (Ron et al. 1984). Eruptions of the Cover Basalt originated in flat, ellipsoid-shaped, NNW–SSE-trending volcanic cones in the Golan Heights (Mor 1986), at the edge of the large NW-trending Harrat Ash-Shaam volcanic field in Jordan. The location of these cones was probably dictated by the tectonic evolution of the Dead Sea fault (Heimann et al. 1996). Cover Basalt that erupted in the Korazim Heights had not erupted during the Early Pliocene in adjacent areas to the east and west (restoring 25–30 km along the eastern marginal fault), so these basalt flows may have been channeled along active faults (Weinstein 2012).

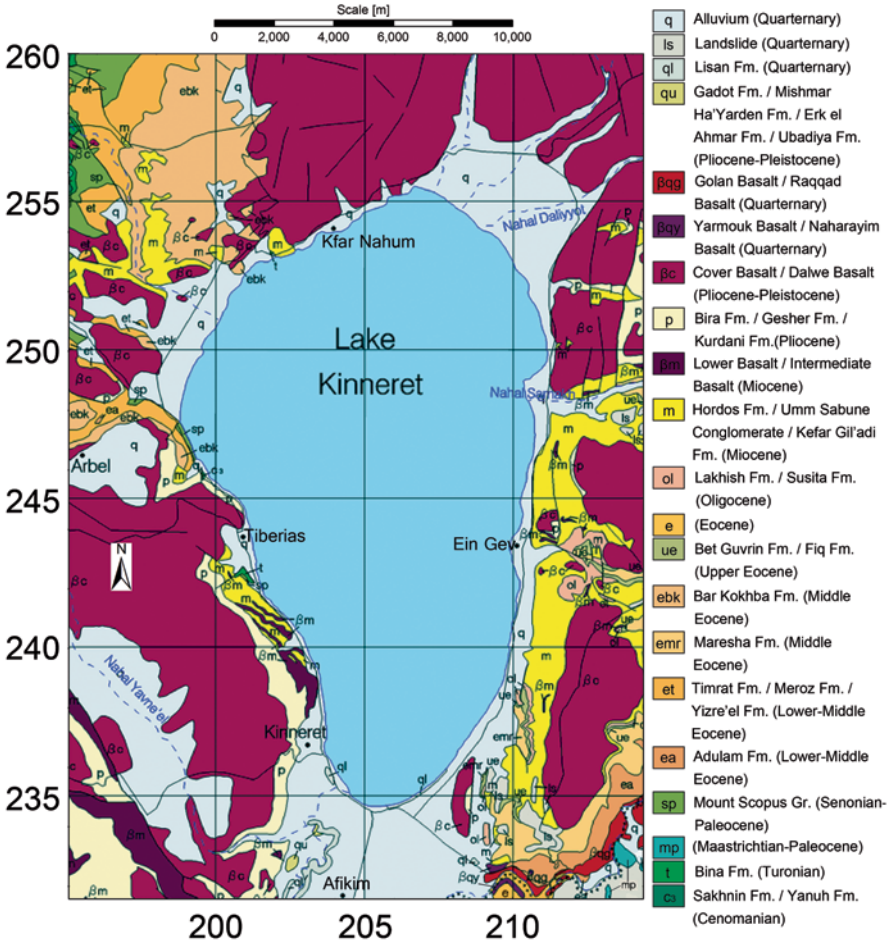

Fig. 2.2 The geology of the surrounding land area of Lake Kinneret. (Modified with permission after the 1:200,000 map of the Geological Survey of Israel; Sneh et al. 1998)

Previous studies of the sub-bottom structure of the lake were carried out using various methods, including seismic reflection and refraction (Ben-Avraham et al. 1981; Ben-Avraham et al. 1986; Ben-Gai and Reznikov 1997; Hurwitz et al. 2002; Reznikov et al. 2004; Ben-Gai 2009), magnetics (Ben-Avraham et al. 1980; Ginzburg and Ben-Avraham 1986), bathymetry (Ben-Avraham et al. 1990), heat flow (Ben-Avraham et al. 1978), and gravity (Ben-Avraham et al. 1996). Although these studies have increased our understanding of the sub-bottom structure of the lake, several key questions remain unsolved: the accurate geometry of the plate boundary in the Lake Kinneret area, the deep sub-bottom structure, the geometry and nature of transverse faulting, and the mechanism controlling the location of submarine springs on the floor of the lake.

Recent studies of the sub-bottom structure of the lake include bathymetry, seismic reflection, magnetics, and seismicity. In these studies, new advanced

instrumentation was used, and the research is ongoing. In this chapter, the main findings of the previous and recent studies will be described and their contribution to the understanding of the structure and evolution of this area will be discussed.

2.2 Bathymetry

The first bathymetric survey of Lake Kinneret was carried out between 1960 and 1970 by TAHAL (Water Planning for Israel). This was followed by a bathymetric survey performed by Ben-Avraham et al. (1990) in 1986 and 1987. The survey was conducted along a grid of N–S and E–W lines with 100-m spacing, and revealed several features. A bathymetric depression, situated >250 m below sea level, occupies the northeastern part of the lake. High gradient slopes are observed mainly along the lake margins, while most of the lake center is associated with a relatively smooth floor. A prominent exception is a steep bathymetric scarp in the southern portion of the lake around latitude 32°45′N (Fig. 2.7). The steep bathymetric slopes might indicate a recent active faulting in the lake that manages to overcome its high sedimentation rates of 2–7 mm year^{-1} (Serruya 1973; Inbar 1976).

The bathymetric data collected by Ben-Avraham et al. (1990) were analyzed in later works (Belitzky and Ben-Avraham 2004; Guitton and Claerbout 2004). In a morphotectonic analysis performed by Belitzky and Ben-Avraham (2004), systematic seafloor disturbances and irregularities were detected and referred to as morpholineaments. Major morpholineaments indicate several kinematic processes: active deformation associated with strike–slip movement along N–S segments of the Dead Sea fault system and normal faulting of the secondary NW–SE to W–E-trending fault system.

A high-resolution bathymetric survey was performed in 2008 with a 4-m grid spacing, using a multibeam system (Tibor and Sade 2009; Sade et al. 2009). Processes of both erosion and accumulation seem to take place in different parts of the lake during the two recent decades, since the previous mapping. Further results based on the recent data are presented and discussed by in Chap. 4.

2.3 Sub-Bottom Structure

2.3.1 Deep Section

2.3.1.1 Magnetic Pattern

A magnetic survey in Lake Kinneret was first carried out by Ben-Avraham et al. (1980). The data were collected with a line spacing interval of 1 km and were analyzed to form a magnetic anomaly map. Its results indicate that the center of the lake is quite smooth in spite of its location at the edge of the large NW-trending Harrat

Ash-Shaam volcanic field in Jordan. Two broad magnetic domains were detected: negative and positive. Both the anomaly domains are trending in E–NE direction, yet the positive anomaly is wider. As opposed to the lake's center, its margins are associated with local anomalies of large amplitude and short wavelength. It is interesting to note that most of the hot salty springs are situated in areas of magnetic anomalies. Apart from basalts, a presence of iron in the surface sediments (Serruya 1971) was suggested as a potential source to the magnetic anomalies (Ben-Avraham et al. 1980). Iron in the form of greigite (Fe_3S_4) was found in sediments of Late Pleistocene age and is thought to affect both the magnetic intensity and the direction of magnetization (Ron et al. 2007).

Magnetic anomalies exist along the northwestern margin of the lake more than in any other part of it (Ben-Avraham et al. 1980). The largest amplitude magnetic anomaly, more than 500 nT, was detected in the northern marginal area near the inflow of the Jordan River into the lake. In the southernmost portion of the lake, there is a significant change in the field pattern, which was later interpreted as a buried basaltic plate dipping from NE to SW at 10° Eppelbaum et al. 2004a; Eppelbaum et al. 2004b; Eppelbaum et al. 2007).

Additional magnetic measurements were performed by Ginzburg and Ben-Avraham (1986), both in the southern part of the lake and farther south on land. The magnetic pattern in these areas revealed that the anomalous zone along the margins of the lake continues onto the land area to the south. Large amplitude anomalies are elongated and aligned along known faults on land, and some of them can be correlated with basalt outcrops. Data interpretation suggests that the main occurrences are of narrow intrusive bodies reaching great depths, such as dykes with associated sills. It seems that several of these bodies form linear features extending southward from the southwestern margin of the lake and then bend to the east, forming the western and southern boundaries of the Kinarot Valley south of the lake.

A recent high-resolution magnetic survey was conducted in 2008 along more than 2,400 km of dense (100 m spacing) grid lines (Tibor and Sade 2009). Analyses of the data produced a new magnetic anomaly map (Fig. 2.3). A comparison between the previous survey and the recent survey revealed general similarities and some new information. Both the magnetic maps show the smooth magnetic domains at the center of the lake: positive in the east (corresponds to normal magnetization) and negative in the north and west (probably corresponds to reverse magnetization). Nevertheless, along the shores of the lake, there are large amplitude anomalies of shorter wavelength, in particular, along the northern shore, where the largest anomalies occur.

2.3.1.2 Gravity

Gravimetric survey was performed in Lake Kinneret by Ben-Avraham et al. (1996). A total of 300 km of continuous marine gravity data were collected in the lake and integrated with land gravity data over 20 km around the lake. The data analysis resulted in gravity anomaly maps and profiles.

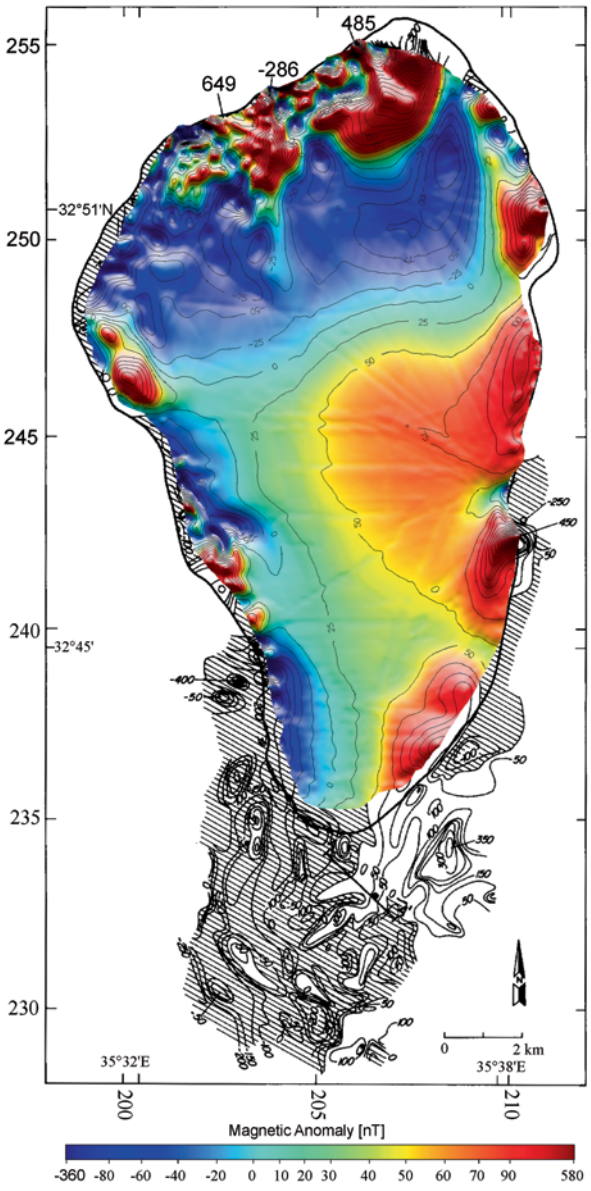

Fig. 2.3 Magnetic anomaly map of Lake Kinneret basin. The marine data are recently obtained (Tibor and Sade 2009) and contoured with an interval of 25 nT. The data on land, south to the lake, with permission after Ginzburg and Ben-Avraham (1986), are contoured with an interval of 50 nT. Areas of negative magnetic anomalies are marked with *diagonal hatching*

The regional and local free-air anomaly maps coincide with the topographic nature of the area: a negative anomaly over the lake itself (−40 mgal) and a positive anomaly (120 mgal) over its surrounding highlands. The negative anomaly is located at the eastern side of the lake, south of the bathymetric depression and along a steep topographic escarpment. In the west, the free-air anomaly drops from the land to the lake margin by about 100 mgal.

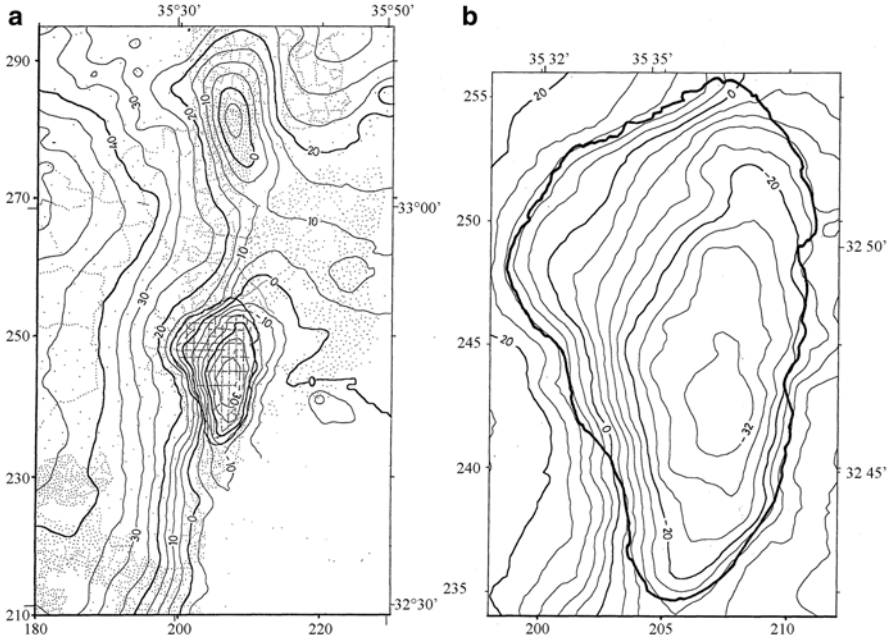

Fig. 2.4 Bouguer gravity anomaly maps of Lake Kinneret (Ben-Avraham et al. 1996): **a** Regional—showing locations of gravity stations (*dots* on land and *lines* in the lake). The gravity values were gridded at 0.65-km square cell size and smoothed. Density used for the Bouguer correction is 2,550 kg m^{-3} above 150 m below sea level (mbsl) and 2,150 kg m^{-3} below 150 mbsl. Reference level for map and lake level during the experiment is 210.2 mbsl. Contour interval is 5 mgal. The Kinneret and Hula basins are clearly expressed on the map. **b** Local—the gravity values were gridded at 0.2-km square cell size and smoothed. Contour interval is 4 mgal. The gravimetric low is located at the southern part of the lake. (Reproduced with permission from Ben Avraham et al. 1996)

Much like the free-air anomaly maps, both the regional and local Bouguer anomaly maps (Fig. 2.4a, b) reveal a prominent gravity low (below −30 mgal) in the southern part of the lake. On the western margin of the Lake Kinneret basin, the values decrease eastward from about 40 mgal to values around 0 mgal. The contour lines do not define clearly the northeastern margin of the lake in any of the maps.

The gravity pattern shown on these maps, together with modeling along E–W gravity profiles, suggests that the Lake Kinneret basin is actually composed of two different structural units, north and south of the latitude 32°49′N. The northern subbasin is asymmetric to the east, and it is wider than the deep southern elongated subbasin. Two N–S boundary faults delimit the southern subbasin: eastern and western. Other geophysical evidence (Fig. 2.5) suggests that these are strike–slip faults (see subsequent discussion).

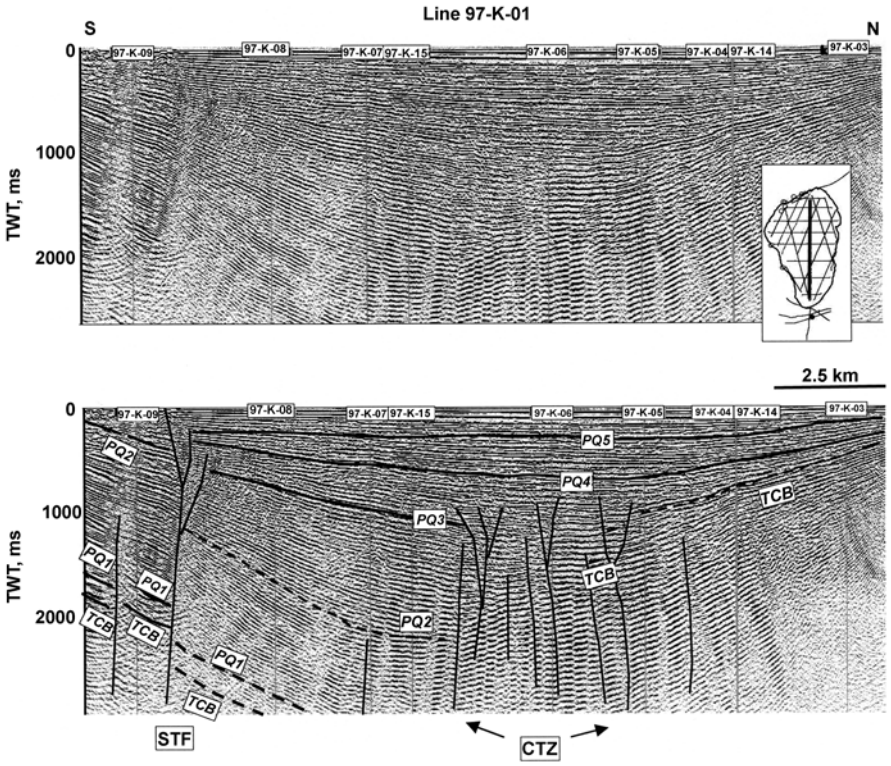

Fig. 2.5 Migrated seismic line 97-K-01 (*top*) and its interpretation (*bottom*) in the Lake Kinneret, reproduced with permission from Reznikov et al. (2004). Southern transverse fault (STF) and central transverse fault zone (CTZ) are southern and central transverse fault zones bordering the deep southern subbasin (Fig. 2.6). *TCB*—top of the Cover Basalt Complex; *PQ*—middle-upper pliocene-quaternary unconformities

2.3.2 Shallow Section

The lake and its surroundings were mapped in previous studies using seismic reflection and refraction surveys (Ben-Avraham et al. 1981; Ben-Avraham et al. 1986; Ben-Gai and Reznikov 1997; Tibor et al. 2004; Reshef et al. 2007). The survey conducted by Ben-Avraham et al. (1981) included several instruments with various frequency bands ranging between few tens to few hundreds of hertz. Despite the poor penetration, evidence of active tectonics, such as folds and faults, was revealed in the uppermost sediments, as well as in the deepest portion of the lake. The next seismic survey was performed with a system of 3.5 kHz (Ben-Avraham et al. 1986). These results showed some bathymetric irregularities, which indicate active tectonic processes that overcome the high sedimentation rate. Using a higher frequency also revealed some zones of increased acoustic penetration: the terrace in the southern part of the lake and areas in the vicinity of hot, salty submarine springs.

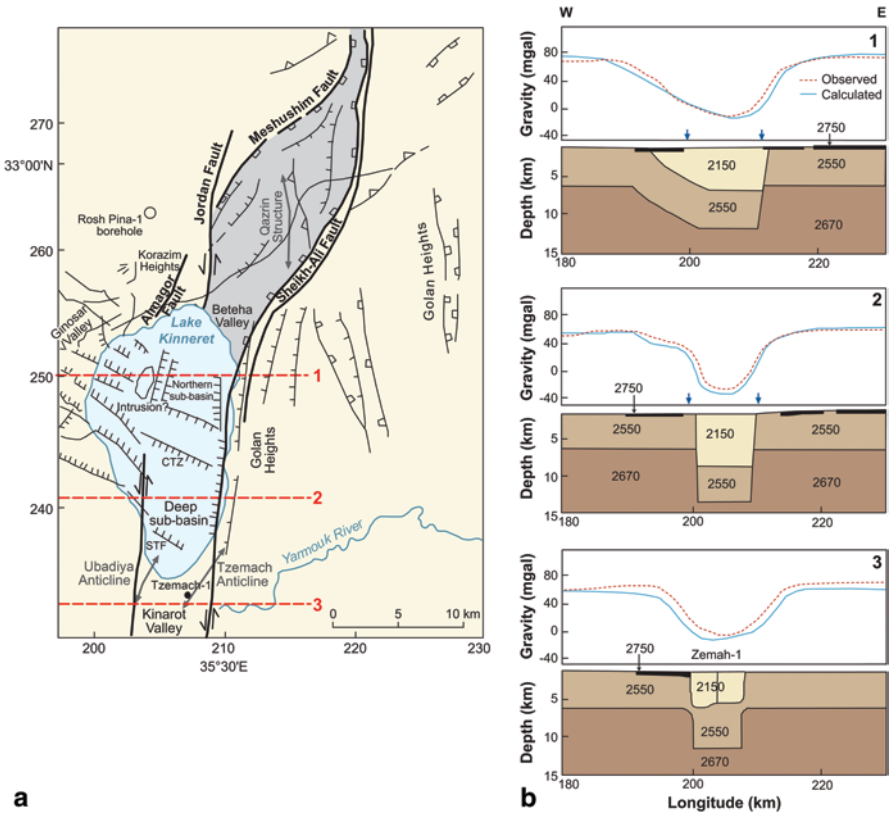

Fig. 2.6 **a** Tectonic map of Lake Kinneret and the Golan Heights based on Ben-Avraham et al. (1996), Hurwitz et al. (2002), Reznikov et al. (2004), and Shulman et al. (2004). *Bold lines* indicate major faults. *Gray area* shows the extent of the Yehudiyya transtensional zone. Major subsurface faults are marked by *squares* and subsurface thrust-faults by *triangles*. *Dashed red lines* (and *numbers*) indicate the location of gravity profiles presented in Fig. 2.6b. STF and CTZ are southern and central transverse fault zones, respectively, bordering the deep southern subbasin. **b** Three E–W gravity profiles (*dashed red lines*) extracted from the free air gravity data, after removal of linear trends, compared with calculated gravity (*solid blue lines*) from two-dimensional density–depth models presented below profiles (based on Ben-Avraham et al. 1996). Location of profiles is shown in Fig. 2.6a. Numbers are densities in kg m^{-3}. *Black layers* represent basalt flows. *Blue arrows* mark the boundaries of the lake. (Modified with permission from Ben-Avraham et al. 2008)

Poor acoustic penetration through most of the lake is caused either by gas presence in the surface sediments (Ben-Avraham et al. 1986) or by homogeneous lithology of fine-grained materials such as silt and clay (Tibor et al. 2004; Reshef et al. 2007).

A multi-channel survey helped in mapping the sub-bottom structure of the lake (Ben-Gai and Reznikov 1997; Hurwitz et al. 2002; Reznikov et al. 2004; Ben-Gai 2009). The presence of dominant N–S-trending longitudinal marginal faults had been suggested by Hurwitz et al. (2002). According to these authors, these steep faults define the boundaries of a large graben that underlies most of the lake. Under

its northwestern part lies another distinct structural zone of pre-rift units at shallow depths. Transverse faults were not observed by Hurwitz et al. (2002), except for the Kfar Nahum fault, which is probably the northern boundary of the Lake Kinneret basin. The eastern marginal fault may be a continuation of the on-land marginal fault in the south (Rotstein et al. 1992). It extends to the northern part of the lake as well, and then continues on land as the Sheikh-Ali fault in the Golan Heights (Fig. 2.6a).

The western marginal fault is also an extension of the on-land fault to the south of the lake, and according to the model proposed by Hurwitz et al. (2002) it crosses its northern part as well. Reznikov et al. (2004) suggested a different model in which the northern continuation of the western marginal fault is a possible part of a large deformation zone under the northwestern part of the lake. The southern part of the lake is occupied by a deep subbasin, which is delimited by the central transverse fault zone (CTZ) and the southern transverse fault (STF) observed in the seismic data (Fig. 2.5). Further features proposed by Reznikov et al. (2004) include a zone of distortion that underlies the central part of the lake, and a possible intrusion in the northwestern part of the lake. Ben-Gai (2009) found no evidence for the southern transverse fault proposed by Reznikov et al. (2004).

2.4 Active Tectonics

The fault geometry in the Lake Kinneret basin includes both longitudinal boundary faults and transverse faults. Steep N–S-trending marginal faults border structural features in the basin (Hurwitz et al. 2002). The eastern marginal fault extends along the northern and southern parts of the lake and continues on land in both directions (Fig. 2.6a): in the north as the Sheikh-Ali fault in the Golan Heights (Shulman et al. 2004) and in the south into the Kinarot Valley (Rotstein et al. 1992; Hurwitz et al. 2002; Reznikov et al. 2004). The western marginal fault extends along the southern part of the lake and continues southward into the Kinarot Valley (Hurwitz et al. 2002; Reznikov et al. 2004). It is unclear whether the western marginal fault extends all the way to the north (Hurwitz et al. 2002) or only up to the point where it meets a complex deformation zone in the northwestern part of the lake (Reznikov et al. 2004). Transverse faults may exist in the northernmost portion of the lake (Hurwitz et al. 2002); however, it is unclear whether they exist in its central and southern parts (Reznikov et al. 2004) or not (Hurwitz et al. 2002; Ben-Gai 2009). Normal faults have been active in the Plio–Pleistocene, keeping up with, and even exceeding sediment accumulation in the Lake Kinneret basin (Marco et al. 2005).

Dramatic variations of the deep sub-bottom structure, based on gravity modeling, occur over different parts of Lake Kinneret (Fig. 2.6b) and explain its unique shape. Based on these variations, the Lake Kinneret basin is divided into two subbasins: northern and southern (Ben-Avraham et al. 1996).

The northern subbasin is a bathymetric depression (Ben-Avraham et al. 1990) occupied by an asymmetric half-graben delimited to the east by the eastern marginal

fault, and to the west by the large deformations suggested by Reznikov et al. (2004). The half-graben structure of a ~6-km sedimentary fill is considered to be an actively subsiding young feature, and it might have been formed due to rotational opening (similar to the one observed in the Korazim Heights and the eastern Galilee by Ron et al. (1984) and Heimann and Ron (1993); see discussion further) and transverse normal faulting, caused by interactions between the two fault systems: the N–S-trending Dead Sea fault and the secondary NW–SE to W–E-trending fault system (Ben-Avraham et al. 1996).

The southern subbasin is a gravimetric depression occupied by a symmetric graben (Ben-Avraham et al. 1996), and it is a deep structure filled with 5–8 km of post-rift sediments with little or no tectonic activity. Sediments of Pleistocene age in the southern subbasin are dipping northward as a result of the active subsidence in the northern subbasin (Ben-Gai 2009). It is unclear whether the graben is delimited in the south by another transverse fault (Reznikov et al. 2004), or whether it extends southward into the Kinarot Valley (Ginzburg and Ben-Avraham 1986; Ben-Avraham et al. 1996; Ben-Gai 2009). The pull-apart graben probably formed as a result of the transform movement along the main strike–slip faults (Freund et al. 1968; Freund 1978; Ginzburg and Ben-Avraham 1986; Hurwitz et al. 2002).

The regional tectonic background in the area can be deciphered (Fig. 2.6a) from features in the vicinity of the Lake Kinneret basin. North to Lake Kinneret, the Korazim Heights is an uplifted block. It may have formed as the block was rotated 11° counterclockwise due to a compressional component that interacted with the geometric relations between the N–S-trending Dead Sea fault and the 20° striking Almagor fault (Heimann and Ron 1993). Therefore, the Korazim Heights is thought to be either a push-up structure (Rotstein and Bartov 1989) or a result of the shortening caused by the compression across the Almagor fault and the uplift of Korazim Heights, which resulted from a block rotation on the inclined Jordan fault (Ben-Avraham et al. 1996). However, the active segment of the Dead Sea fault in this area seems to be along the Jordan fault, rather than the Almagor fault (Marco et al. 2005).

Northeast of Lake Kinneret, the basin continues into the NE–SW Yehudiyya transtensional zone. In its southwestern part, the Beteha Valley is an area of both strike–slip motion along the Jordan fault (Marco et al. 2005) and dip–slip motion towards the deep depression in the northern subbasin of Lake Kinneret (Shulman et al. 2004). The highly faulted Yehudiyya extension zone was formed by the activity of the NE-branching Sheikh-Ali and Meshushim faults from the Dead Sea fault (Fig. 2.6a). This structure probably existed at the time of the Upper Pliocene to Pleistocene basalt eruptions and controlled their flow direction (Shulman et al. 2004).

Paleoseismic studies and archeological sites provide evidence for active tectonics all around Lake Kinneret (Marco 2008; Marco et al. 2005). An active NW–SE fault bisecting the city of Tiberias (Fig. 2.2) was proposed by Marco et al. (2003). Landslides were documented along fault lineaments both east and west of the lake (Katz et al. 2009; Yagoda-Biran et al. 2010).

South of Lake Kinneret, within the Kinarot Valley, the Tzemach−1 (4,249 m) well (Fig. 2.6a), which penetrated a Miocene-to-Late Pleistocene sequence, provides direct evidence for the subsurface composition of the area: limestones, marls, conglomerates, salt, and igneous rocks (Marcus and Slager 1985). These strata filled the Kinarot Valley more than 4 km as it accumulated at rates exceeding 1.5 mm year^{-1} both during the Late Miocene (Horowitz 1987) and between 2.2 and 2 Ma ago (Horowitz 1989; Braun et al. 1991), but at much lower rates ever since (Horowitz 1987, 1989). The subsidence rate since the Pliocene is thought to be 0.12–0.24 mm year^{-1} (Shaliv 1991; Mor 1993). The Kinarot Valley is a possible extension of the southern subbasin (Ben-Avraham et al. 1996; Ginzburg and Ben-Avraham 1986). The NE–SW-trending Tzemach anticline is an uplifted structure in the eastern part of the Kinarot Valley. Rotstein et al. (1992) suggested the presence of a reverse fault that accommodated the Tzemach anticline and acted until the Late Quaternary. According to Ben-Gai (2009), the Tzemach structure is actually a diapir consisting of thick evaporitic section deposited during the Late Miocene and Early Pliocene, when it might have been located in the deepest part of the Kinneret-Beit Shean basin. Upwelling of the Tzemach structure intensifies the dipping of sediments in the southern subbasin as a result of the subsidence in the northern subbasin (Ben-Gai 2009).

2.5 Seismicity

The complex structure of Lake Kinneret basin consists of numerous fault segments in different orientations. The geometry and nature of these faults have not been mapped and deciphered completely. Since the Lake Kinneret basin is part of the seismically active Dead Sea fault, these fault segments generate low-intensity seismicity. The destructive damage that the area has suffered is evident in the local geology and morphology as well as in historical writings and archeological ruins (e.g., Segal et al. 2002; Marco 2008; Wechsler et al. 2009). However, the evident damage was caused by rare strong earthquakes of magnitude greater than $M_S = 7$ (Ambraseys and Barazangi 1989; Ambraseys and Jackson 1998; Ellenblum et al. 1998; Marco et al. 2003, 2005), whose epicenters originated far from the Lake Kinneret basin. Instrumental recording since 1900 shows that the greatest earthquake located within the Lake Kinneret basin was not more than $M_L = 4.5$ (Israeli earthquake catalog from the Geophysical Institute of Israel, GII).

Since Lake Kinneret basin occupies a relatively small area, seismological studies do not refer to it as an independent seismogenic zone but only as part of a greater zone such as the Jordan Valley or the Hula Valley. Previous investigations of the seismicity along segments of the Dead Sea fault reveal that the microearthquakes in the Lake Kinneret basin have a tendency to cluster in space (van Eck and Hofstetter 1990). Focal plane solutions, which were calculated for a number of events within the Lake Kinneret basin, show that the mechanism of the microseismic activity in Lake Kinneret basin is in agreement with the orientation of the transform movement

(van Eck and Hofstetter 1990), but could also have different orientations, which do not always agree with related faults on land (Hofstetter et al. 2007). The calculated *b-value* of the northern segment of the Dead Sea fault fluctuates between 0.8 and 0.86 (Ben-Menahem 1981, 1991; Shapira and Feldman 1987), which is lower than the *b-value* of 0.96 which was calculated for the total Dead Sea fault (Shapira 2002, Appendix C). An interesting observation was made by Kafri and Shapira (1990), who suggested that the recorded seismic activity in the Kinneret region might be related to the water level of the lake and rainfalls. A correlation between the occurrences of felt earthquakes and both the beginning of the rainy season and the annual minimum water level was found. This correlation was explained as a process in which frictional strength along the boundary faults of the Dead Sea fault is reduced by upward flows, triggering an earthquake that would have occurred later due to the tectonic stress.

2.5.1 Microseismic Catalog

In order to characterize the local microseismic events which are generated in the Lake Kinneret basin area, a highly sensitive Seismic Navigation System (SNS) was deployed in the basin area (Navon 2011). During 2010, a cluster of four portable mini-arrays installed in Korazim, Almagor, Ma'ale Gamla, and Ramot (Fig. 2.7) recorded data in a continuous mode at sampling rate of 250 Hz. Within 9 months, the deployment of the SNS has enabled the detection of 121 earthquakes with a magnitude threshold of $M_L = -1.2$. The high sampling rate has enabled to record full signal spectra and to determine their corner frequencies. The results show rather high values of the displacement signals ranging between 7 and 20 Hz.

2.5.2 Implications of Microseismic Data of Different Time Scales

The new catalog, obtained by the SNS, is compared to the local catalog of earthquakes detected over 25 years by the GII (Navon 2011). Both catalogs show that most of the microseismic activity is concentrated in the northern portion of the Lake Kinneret basin (Fig. 2.7). The events in both catalogs are characterized by very low magnitudes, and most of them display shallow hypocentral depths above 12 km deep. The *b-value* that was calculated for the GII catalog was $b = 0.82$, which is in accordance with results achieved in previous studies. The *b-value* calculated for the SNS catalog ($b = 0.65$) is significantly lower and might indicate high stress regime or temporal changes in the stress regime. Both catalogs reveal the tendency to cluster in time and space in the northern subbasin of the Lake Kinneret basin.

Although the data are still too sparse to map the geometry of the Lake Kinneret basin faults with accuracy, the new SNS catalog supplemented by the GII catalog displays seismicity that can be associated with existing tectonic features (Fig. 2.6a). The Jordan fault is presently active, but there is still no evidence showing how its

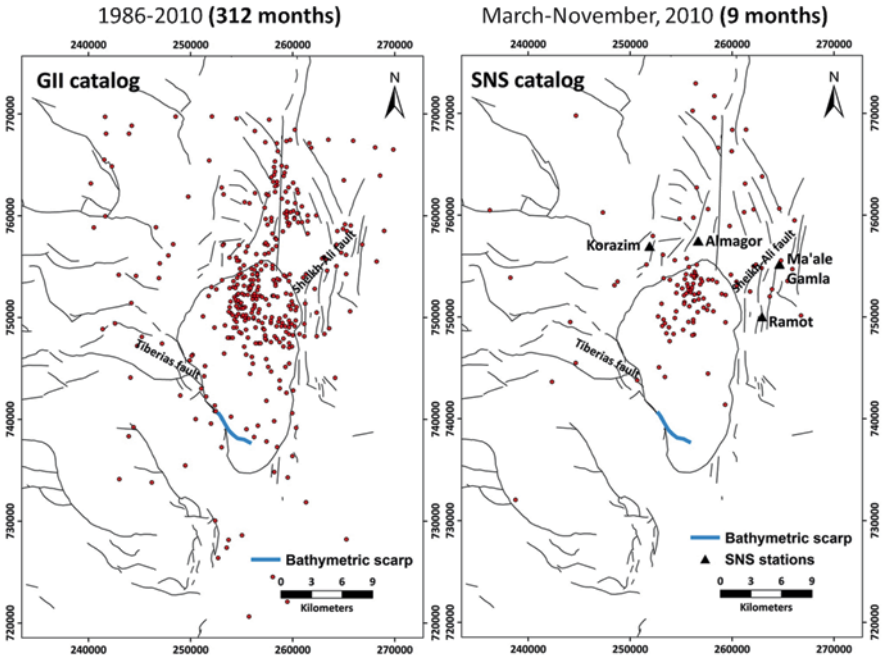

Fig. 2.7 Spatial distribution of seismic activity in the Lake Kinneret basin as observed by the Geophysical Institute of Israel, GII (*left*) and the Seismic Navigation System, SNS (*right*). The deployment of the SNS has enabled the detection of a large amount of earthquakes in a short period of time. Comparing the results of the GII catalog and the SNS catalog displays a rather similar behavior of seismic activity. (Navon 2011)

southern extent connects to the boundary faults of the Dead Sea fault within the Lake Kinneret basin. The northern subbasin is the most seismically active feature, possibly confirming the hypothesis of Ben-Avraham et al. (1996) that it is currently subsiding. The distribution of events in that subbasin also supports the claim that it is highly deformed (Reznikov et al. 2004). Several earthquake clusters, which were observed in the northern subbasin, seem to delimit its borders and indicate that the Lake Kinneret basin functions as a barrier to the movement of the Dead Sea fault in this section (Sibson 1985; van Eck and Hofstetter 1990; Ben-Avraham et al. 1996). The enhanced seismicity along the bathymetric scarp in the southern part of the lake (Fig. 2.7) supports the claim of Ben-Avraham et al. (1990) and Reznikov et al. (2004) that this could be an expression of an active fault line that may be the offshore extension of the active Tiberias fault (Fig. 2.7) The Sheikh-Ali fault (Fig. 2.7) shows moderate seismicity and the absence of seismic activity south of Lake Kinneret suggests that it may be a locked segment of the Dead Sea fault.

2.6 Conclusions

The intricate sub-bottom structure of the Lake Kinneret basin derives from a complex geological history of various tectonic processes that go back to the Neogene. The main tectonic processes are the intersection of the Dead Sea fault system with a NW–SE to W–E-trending fault system crossing the Galilee, combined with the Taurus–Zagros plate collision zone farther north (Fig. 2.1).

The Lake Kinneret basin is divided into two structural units, each associated with a different mechanism of formation. Rotational opening and transverse normal faulting are possibly responsible for the asymmetric half-graben occupying the northern subbasin. The symmetric graben occupying the southern subbasin is the deepest part of the basin, and may have been formed due to pull-apart opening caused by the transform movement along the main segments of the Dead Sea fault.

Active tectonics is taking place across the Lake Kinneret basin and is evident both in morphological features and in recent seismicity. The N–S marginal faults are associated with strike–slip motion, while transverse faults have a main vertical component causing a normal dip–slip motion. The most tectonically active zone is the northern subbasin, which is actively subsiding and forms the bathymetrically deepest part of the lake.

References

Ambraseys NN, Barazangi M (1989) The 1759 earthquake in the Bekaa Valley: implications for earthquake hazard assessment in the Eastern Mediterranean region. J Geophys Res 94(B4):4007–4013. doi:10.1029/JB094iB04p04007

Ambraseys NN, Jackson JA (1998) Faulting associated with historical and recent earthquakes in the Eastern Mediterranean region. Geophys J Int 133(2):390–406. doi:10.1046/j.1365–246X.1998.00508.x

Belitzky S, Ben-Avraham Z (2004) The morphotectonic pattern of Lake Kinneret. Isr J Earth Sci 53(3):121–130. doi:10.1560/YUXY-8DMJ-85B4-GMH7

Ben-Avraham Z, Hänel R, Villinger H (1978) Heat flow through the Dead Sea rift. Mar Geol 28(3–4):253–269. doi:10.1016/0025–3227(78)90021-X

Ben-Avraham Z, Shoham Y, Klein E, Michelson H, Serruya C (1980) Magnetic survey of Lake Kinneret-central Jordan Valley, Israel. Mar Geophys Res 4(3):257–276. doi:10.1007/bf00369102

Ben-Avraham Z, Ginzburg A, Yuval Z (1981) Seismic reflection and refraction investigations of Lake Kinneret-central Jordan Valley, Israel. Tectonophysics 80(1–4):165–181. doi:10.1016/0040–1951(81)90148–7

Ben-Avraham Z, Shaliv G, Nur A (1986) Acoustic reflectivity and shallow sedimentary structure in the Sea of Galilee—Jordan Valley. Mar Geol 70(3–4):175–189. doi:10.1016/0025–3227(86)90001–0

Ben-Avraham Z, Amit G, Golan A, Begin ZB (1990) The bathymetry of Lake Kinneret and its structural significance. Isr J Earth Sci 39(2/4):77–84

Ben-Avraham Z, ten Brink US, Bell R, Reznikov M (1996) Gravity field over the Sea of Galilee: evidence for a composite basin along a transform fault. J Geophys Res 101(B1):533–544. doi:10.1029/95JB03043

Ben-Avraham Z, Garfunkel Z, Lazar M (2008) Geology and evolution of the southern Dead Sea fault with emphasis on subsurface structure. Annu Rev Earth Planet Sci 36:357–387. doi:10.1146/annurevearth.36.031207.124201

Ben-Gai Y (2009) Subsurface geology of the southern Lake Kinneret (Sea of Galilee), Dead Sea transform—evidence from seismic reflection data. Isr J Earth Sci 58(3):163–175. doi:10.1560/ijes.58.3–4.163

Ben-Gai Y, Reznikov M (1997) Multi-channel seismic survey in the Sea of Galilee. Geophysical Institute of Israel, Holon

Ben-Menahem A (1981) Variation of slip and creep along the Levant rift over the past 4500 years. Tectonophysics 80(1–4):183–197. doi:10.1016/0040–1951(81)90149–9

Ben-Menahem A (1991) Four thousand years of seismicity along the Dead Sea rift. J Geophys Res 96(B12):20195–20216. doi:10.1029/91jb01936

Braun D, Ron H, Marco S (1991) Magnetostratigraphy of the hominid tool-bearing Erk el Ahmar formation in the northern Dead Sea rift. Isr J Earth Sci 40:191–197

Braun Y, Kagan E, Bar-Matthews M, Ayalon A, Agnon A (2009) Dating speleoseismites near the Dead Sea transform and the Carmel fault: clues to coupling of a plate boundary and its branch. Isr J Earth Sci 58(3):257–273. doi:10.1560/ijes.58.3–4.257

Ellenblum R, Marco S, Agnon A, Rockwell T, Boas A (1998) Crusader castle torn apart by earthquake at dawn, 20 May 1202. Geology 26(4):303–306. doi:10.1130/0091–7613 (1998) 026<0303:cctabe>2.3.co;2

Eppelbaum L, Ben-Avraham Z, Katz Y (2004a) Integrated analysis of magnetic, paleomagnetic and K–Ar data in a tectonic complex region: an example from the Sea of Galilee. Geophys Res Lett 31(19). doi:10.1029/2004GL021298

Eppelbaum L, Ben-Avraham Z, Katz Y, Marco S (2004b) Sea of Galilee: comprehensive analysis of magnetic anomalies. Isr J Earth Sci 53(3):151–171. doi:10.1560/NQUR-CR5M-AQQX-KX1A

Eppelbaum L, Ben-Avraham Z, Katz Y (2007) Structure of the Sea of Galilee and Kinarot Valley derived from combined geological–geophysical analysis. First Break 25:21–28

Freund R (1970) The geometry of faulting in the Galilee. Isr J Earth Sci 19(3–4):117–140

Freund R (1978) The concept of a sinistral megashear. In: Serruya C (ed) Lake Kinneret. Monographiae biologicae, vol 32. Dr W. Junk bv Publishers, The Hague, pp 27–31

Freund R, Oppenheim MJ, Schulman N (1965) Direction of magnetization of some basalts in the Jordan Valley and Lower Galilee (Israel). Isr J Earth Sci 14(2):37–44

Freund R, Zak I, Garfunkel Z (1968) Age and rate of the sinistral movement along the Dead Sea rift. Nature 220(5164):253–255

Garfunkel Z (1981) Internal structure of the Dead Sea leaky transform (rift) in relation to plate kinematics. Tectonophysics 80(1–4):81–108. doi:10.1016/0040–1951(81)90143–8

Garfunkel Z, Ben-Avraham Z (2001) Basins along the Dead Sea transform. In: Ziegler PA, Cavazza W, Robertson AHF, Crasquin-Soleau S (eds) Peri-Tethyan rift/wrench basins and passive margins, vol 186 (Peri-Tethys Memoir, vol 6). Mémoires du Muséum national d'histoire naturelle, Paris, pp 607–627

Ginzburg A, Ben-Avraham Z (1986) The structure of the Sea of Galilee graben, Israel, from magnetic measurements. Tectonophysics 126(2–4):153–164. doi:10.1016/0040–1951(86)90225–8

Guitton A, Claerbout J (2004) Interpolation of bathymetry data from the Sea of Galilee: a noise attenuation problem. Geophysics 69(2):608–616. doi:10.1190/1.1707081

Heimann A (1990) The development of the Dead Sea rift and its margins in northern Israel during the Pliocene and the Pleistocene, PhD thesis. Hebrew University, Jerusalem

Heimann A, Ron H (1993) Geometric changes of plate boundaries along part of the northern Dead Sea transform: geochronologic and paleomagnetic evidence. Tectonics 12(2):477–491. doi:10.1029/92tc01789

Heimann A, Steinitz G, Mor D, Shaliv G (1996) The cover basalt formation, its age and its regional and tectonic setting: implications from K-Ar and (40)Ar-(39)Ar geochronology. Isr J Earth Sci 45(2):55–71

Hofstetter R, Klinger Y, Amrat A-Q, Rivera L, Dorbath L (2007) Stress tensor and focal mechanisms along the Dead Sea fault and related structural elements based on seismological data. Tectonophysics 429(3–4):165–181. doi:10.1016/j.tecto.2006.03.010

Horowitz A (1987) Palynological evidence for the age and rate of sedimentation along the Dead Sea rift, and structural implications. Tectonophysics 141(1–3):107–115. doi:10.1016/0040–1951(87)90178–8

Horowitz A (1989) Palynological evidence for the quaternary rates of accumulation along the Dead Sea rift, and structural implications. Tectonophysics 164(1):63–71. doi:10.1016/0040–1951(89)90234–5

Hurwitz S, Garfunkel Z, Ben-Gai Y, Reznikov M, Rotstein Y, Gvirtzman H (2002) The tectonic framework of a complex pull-apart basin: seismic reflection observations in the Sea of Galilee, Dead Sea transform. Tectonophysics 359(3–4):289–306. doi:10.1016/S0040–1951(02)00516–4

Inbar M (1976) Contemporary and Holocene denudation rates in the Lake Kinneret watershed. In: Amiran D, Ben-Arieh Y (eds) Geography in Israel: a collection of papers offered to the 23rd International Geographical Congress, USSR, July–August, Jerusalem, 1976. Israel National Committee, International Geographical Union, pp 344–352

Kafri U, Shapira A (1990) A correlation between earthquake occurrence, rainfall and water level in Lake Kinnereth, Israel. Phys Earth Planet Inter 62(3–4):277–283. doi:10.1016/0031–9201(90)90172-t

Kashai EL, Croker PF (1987) Structural geometry and evolution of the Dead Sea–Jordan rift system as deduced from new subsurface data. Tectonophysics 141(1–3):33–60. doi:10.1016/0040–1951(87)90173–9

Katz O, Amit R, Yagoda-Biran G, Hatzor Y, Porat N, Medvedev B (2009) Quaternary earthquakes and landslides in the Sea of Galilee area, the Dead Sea transform: paleoseismic analysis and implication to the current hazard. Isr J Earth Sci 58(3):275–294. doi:10.1560/ijes.58.3–4.275

Marco S (2008) Recognition of earthquake-related damage in archaeological sites: examples from the Dead Sea fault zone. Tectonophysics 453(1–4):148–156. doi:10.1016/j.tecto.2007.04.011

Marco S, Hartal M, Hazan N, Lev L, Stein M (2003) Archaeology, history, and geology of the AD 749 earthquake, Dead Sea transform. Geology 31(8):665–668. doi:10.1130/g19516.1

Marco S, Rockwell TK, Heimann A, Frieslander U, Agnon A (2005) Late Holocene activity of the Dead Sea transform revealed in 3D palaeoseismic trenches on the Jordan Gorge segment. Earth Planet Sci Lett 234(1–2):189–205. doi:10.1016/j.epsl.2005.01.017

Marcus E, Slager J (1985) The sedimentary-magmatic sequence of the Zemah-1 well (Jordan–Dead Sea rift, Israel) and its emplacement in time and space. Isr J Earth Sci 34(1):1–10

Michelson H (1972) The hydrogeology of the southern Golan Heights. Tahal—Water Planning for Israel Ltd., Tel-Aviv

Mor D (1986) The volcanism of the Golan Heights, PhD thesis. Hebrew University, Jerusalem

Mor D (1993) A time-table for the Levant volcanic province, according to K-Ar dating in the Golan Heights, Israel. J Afr Earth Sci (and the Middle East) 16(3):223

Mor D, Steinitz G (1982) K-Ar age of the cover basalts surrounding the Sea of Galilee. Geological Survey of Israel, Jerusalem

Navon H (2011) Microseismic characterization of Lake Kinneret basin, MSc thesis. Tel Aviv University, Tel-Aviv

Picard L (1936) Conditions of underground water in the western Emek (plain of Esdraelon). Bull Geol Dep 1:1–23 (Hebrew University)

Picard L (1943) Structure and evolution of Palestine: with comparative notes on neighboring countries. Bull Geol Dep 4:1–187 (Hebrew University)

Reshef M, Ben-Avraham Z, Tibor G, Marco S (2007) The use of acoustic imaging to reveal fossil fluvial systems—a case study from the southwestern Sea of Galilee. Geomorphology 83(1–2):58–66. doi:10.1016/j.geomorph.2006.05.017

Reznikov M, Ben-Avraham Z, Garfunkel Z, Gvirtzman H, Rotstein Y (2004) Structural and stratigraphic framework of Lake Kinneret. Isr J Earth Sci 53(3):131–149. doi:10.1560/QY1W-VVRM-FLNK-C9M9

Ron H, Freund R, Garfunkel Z, Nur A (1984) Block rotation by strike–slip faulting—structural and paleomagnetic evidence. J Geophys Res 89(NB7):6256–6270. doi:10.1029/JB089iB07p06256

Ron H, Nowaczyk NR, Frank U, Schwab MJ, Naumann R, Striewski B, Agnon A (2007) Greigite detected as dominating remanence carrier in late Pleistocene sediments, Lisan formation, from Lake Kinneret (Sea of Galilee), Israel. Geophys J Int 170(1):117–131. doi:10.1111/j.1365–246X.2007.03425.x

Rotstein Y, Bartov Y (1989) Seismic reflection across a continental transform: an example from a convergent segment of the Dead Sea rift. J Geophys Res 94(B3):2902–2912. doi:10.1029/JB094iB03p02902

Rotstein Y, Bartov Y, Frieslander U (1992) Evidence for local shifting of the main fault and changes in the structural setting, Kinarot basin, Dead Sea transform. Geology 20(3):251–254. doi:10.1130/0091–7613 (1992) 020 <0251:eflsot> 2.3.co;2

Sade AR, Tibor G, Hall JK, Diamant M, Sade H, Hartman G, Amit G, Schulze B, Zohary T, Markel D (2009) High resolution multibeam bathymetry of the Sea of Galilee (Lake Kinneret). Isr J Earth Sci 58(2):121–129. doi:10.1560/IJES.58.2.121

Sadeh M, Hamiel Y, Ziv A, Bock Y, Fang P, Wdowinski S (2012) Crustal deformation along the Dead Sea transform and the Carmel fault inferred from 12 years of GPS measurements. J Geophys Res 117(B8):B08410. doi:10.1029/2012jb009241

Saltzman U (1964) The geology of Tabgha, Hukuk and Migdal area, MSc thesis. Hebrew University, Jerusalem

Schulman N (1962) The geology of the central Jordan Valley, PhD thesis. Hebrew University, Jerusalem

Segal A, Mlynarczyk J, Burdajewicz M, Schuler M (2002) Hippos (Sussita), third season of excavations. Zinman Institute of Archaeology, University of Haifa, Haifa

Serruya C (1971) Lake Kinneret: the nutrient chemistry of the sediments. Limnol Oceanogr 16(3):510–521

Serruya C (1973) Sediments. In: Berman T (ed) Lake Kinneret Data Record. Israel National Council for Research and Development, pp 13–73, 39–45

Shaliv G (1991) Stages in the tectonic and volcanic history of the Neogene basin in the lower Galilee and the valleys, PhD thesis. Hebrew University, Jerusalem

Shapira A (2002) An updated map of peak ground accelerations for the Israel Standard 413. Geophysical Institute of Israel, Lod

Shapira A, Feldman L (1987) Microseismicity of three locations along the Jordan rift. Tectonophysics 141(1–3):89–94. doi:10.1016/0040–1951(87)90176–4

Shulman H, Reshef M, Ben-Avraham Z (2004) The structure of the Golan Heights and its tectonic linkage to the Dead Sea transform and the Palmyrides folding. Isr J Earth Sci 53(3):225–237

Sibson RH (1985) Stopping of earthquake ruptures at dilational fault jogs. Nature 316(6025):248–251. doi:10.1038/316248a0

Siedner G, Horowitz A (1974) Radiometric ages of late Cainozoic basalts from northern Israel: chronostratigraphic implications. Nature 250(5461):23–26

Sneh A., Bartov Y, Rosensaft M (1998) Geological map of Israel 1:200,000, sheet 1. Geological Survey of Israel, Jerusalem

Tibor G, Sade AR (2009) Kinneret seabed mapping at high resolution. Israel Oceanographic and Limnological Research Ltd., Haifa

Tibor G, Ben-Avraham Z, Herut B, Nishri A, Zurieli A (2004) Bottom morphology and shallow structures in the northwestern part of Lake Kinneret. Israel Journal of Earth Sciences 53(3):173–186. doi:10.1560/TE15-KU60–6XV3-XK5U

van Eck T, Hofstetter A (1990) Fault geometry and spatial clustering of microearthquakes along the Dead Sea–Jordan rift fault zone. Tectonophysics 180(1):15–27. doi:10.1016/0040–1951(90)90368-i

Walley CD (1998) Some outstanding issues in the geology of Lebanon and their importance in the tectonic evolution of the Levantine region. Tectonophysics 298(1–3):37–62. doi:10.1016/s0040–1951(98)00177–2

Wechsler N, Katz O, Dray Y, Gonen I, Marco S (2009) Estimating location and size of historical earthquake by combining archaeology and geology in Umm-El-Qanatir, Dead Sea transform. Nat Hazards 50(1):27–43. doi:10.1007/s11069–008-9315–6

Weinstein Y (2012) Transform faults as lithospheric boundaries, an example from the Dead Sea transform. J Geodyn 54:21–28. doi:10.1016/j.jog.2011.09.005

Weinstein Y, Navon O, Altherr R, Stein M (2006) The role of lithospheric mantle heterogeneity in the generation of Plio-Pleistocene alkali basaltic suites from NW Harrat Ash Shaam (Israel). J Petrology 47(5):1017–1050. doi:10.1093/petrology/egl003

Yagoda-Biran G, Hatzor YH, Amit R, Katz O (2010) Constraining regional paleo peak ground acceleration from back analysis of prehistoric landslides: example from Sea of Galilee, Dead Sea transform. Tectonophysics 490(1–2):81–92. doi:10.1016/j.tecto.2010.04.029

http://www.springer.com/978-94-017-8943-1

Lake Kinneret
Ecology and Management
Zohary, T.; Sukenik, A.; Berman, T.; Nishri, A. (Eds.)
2014, XVIII, 683 p. 230 illus., 51 illus. in color.,
Hardcover
ISBN: 978-94-017-8943-1